Oxidation of Cr_3Si-Cr_7C_3/SiC/SiC Coated C/SiC Composite in Wet Air

Jinlian Liang
Northwest Agriculture and Forestry University
Shoujun Wu (shoujun_wu@163.com)
Northwest Agriculture and Forestry University
Shaojun Ma
Northwest Agriculture and Forestry University
Ning Dong
Northwestern Polytechnical University

Research Article

Keywords: C/SiC, Cr3Si-Cr7C3, Wet Oxidation, Coating, Flexural strength, Microstructure

Posted Date: June 30th, 2020

DOI: https://doi.org/10.21203/rs.3.rs-39075/v1

Abstract

Oxidation behavior of a Cr_3Si-Cr_7C_3/SiC/SiC coated C/SiC composite was investigated in wet air at 700, 900 and 1300 ºC under 1 atm with a gas velocity of 3.0 cm s^{-1}, and compared with that of a SiC/SiC/SiC coated C/SiC composite. The wet oxidation produced phases on the Cr_3Si-Cr_7C_3/SiC/SiC coating were Cr_2O_3 at 700 and 900 ºC, and Cr_2O_3 and SiO_2 at 1300 ºC. The Cr_3Si-Cr_7C_3/SiC/SiC coating showed enhanced protection against wet oxidation compared to the SiC/SiC/SiC coating. After oxidation for 10 h, the Cr_3Si-Cr_7C_3/SiC/SiC coated composites showed nearly the same failure behavior and residual flexural strength as the as-received composites.

1. Introduction

Continuous carbon fiber reinforced silicon carbide (C/SiC) composites exhibit many excellent properties, such as low density, high specific strength and modulus, high fracture toughness and improved oxidation resistance than carbon/carbon (C/C) composites. Therefore, they are one of the most promising thermostructural materials applied as high temperature structural components such as heat exchangers, hot gas filters, turbine engines, spacecraft reentry thermal protection systems, etc. [1–5]. In certain applications, such as combustor liners, turbine vanes and thrusters for propulsion, the operating environment is a high-temperature oxidizing environment containing water vapor [6]. It has also been demonstrated that water can enhance the oxidation rate of SiC and carbon [7–12]. Therefore, protection of C/SiC composites from oxidation, especially in high temperature water vapor containing oxidizing environments is a concern.

Earlier work has demonstrated that a Cr_3Si-Cr_7C_3 outer layer prepared on CVD SiC coating [13] showed an enhanced oxidation protection in air as compared to a SiC/SiC/SiC coating. However, the effect of the Cr_3Si-Cr_7C_3 outer layer on the wet oxidation of SiC coated C/SiC has not been investigated so far.

In this paper, the high temperature oxidation behavior of a Cr_3Si-Cr_7C_3/SiC/SiC coated C/SiC was investigated in 18 vol. % O_2 + 72 vol. % N_2 + 10 vol. % H_2O under 1 atm and a gas flow rate of 3.0 cm s^{-1} at 700 ºC, 900 ºC and 1300 ºC. The analysis and discussion presented in this paper focus principally on the oxidation mechanisms based on the weight change kinetics, residual flexural strength change and microstructure analysis. A comparison with the corresponding properties of a SiC/SiC/SiC coated C/SiC composite is also presented.

2. Experiment Procedure

2.1. Fabrication of samples

A 2D C/SiC composite, used as the substrate, was prepared by low-pressure chemical vapor infiltration (LPCVI). The preform was piled up with polyacrylonitrile (PAN)-based carbon fiber clothes (T300™). The volume fraction of the fiber preform was controlled in the range of 40–45%. The preform was deposited

with a pyrolytic carbon (PyC) and SiC using butane and methyltrichlorosilane (MTS). An LPCVI process was used to deposit the PyC interphase and the SiC matrix for the composite using butane and MTS, respectively. The deposition conditions for the PyC interface layer were as follows: temperature 960 °C, pressure 5 kPa, time 20 h, Ar flow 200 mL min^{-1}, C_4H_{10} flow 15 mL min^{-1}. The deposition conditions for the SiC matrix were as follows: temperature 1000 °C, pressure 5 kPa, time 120 h, H_2 flow 350 $mLmin^{-1}$, Ar flow 350 $mLmin^{-1}$, and the mole ratio of H_2 to MTS was 10:1. The as-received composite was machined and polished to obtain substrates of dimension of 3.0 mm × 4.0 mm × 30 mm.

The gained composite substrates were initially coated with two layers of SiC by CVD, after which an additional Cr_3Si-Cr_7C_3 coating was added using a Powder Immersion Reaction Assisted Coating (PIRAC) method. And this coating was referred to as Cr_3Si-Cr_7C_3/SiC/SiC coating. The conditions for CVD SiC were the same as that of the SiC matrix, except that the deposition time was 30 h per cycle. In the PIRAC processing, samples with two layers of SiC coatings were first immersed into Cr powders and sealed in a Cr-rich stainless steel container. These were then enclosed in a second stainless steel container with small amounts of titanium and chromium powder that functioned as getters for N_2 and O_2, respectively. The Cr_3Si-Cr_7C_3 coating was prepared at 1000 °C for 2 h [13]. For comparison, samples with three layers of CVD SiC coating (referred to as SiC/SiC/SiC coating) were prepared.

2.2 Oxidation tests

Oxidation tests of the coated C/SiC composites were carried out at 700 °C, 900 °C and 1300 °C under a gas mixture containing 18 vol % O_2 + 72% vol % N_2 + 10 vol % H_2O at 1 atm pressure. Deionized water was used as water vapor source. Three specimens put in an alumina tube with a purity of 99.99% were used for each test. The samples were introduced into a heating furnace at the desired temperature, and the oxidizing mixture was then admitted into the reactor. It has been demonstrated that silica is volatile under operation conditions of a turbine, where high gas velocity along with a high partial pressure of water vapor is used. However, at low gas velocity and low gas pressure, silica volatilization and the corresponding steady-state recession rate are negligible [14]. In the present experiment, the velocity of the gas mixture was maintained at 3.0 cm s^{-1} to minimize the volatility of the SiO_2 scale formed on the SiC coating. The mass of the specimens before and after oxidation were measured using an electronic analytical balance (resolution: 0.01 mg).

2.3. Measurements of the composites

The flexural strength of the samples before and after the wet oxidation was measured by a three-point bending method, which was carried out on an Instron 1195 machine at room temperature. The span dimension was 20 mm and the loading rate was 0.5 mm min^{-1}.

Phase composition and microstructure of the samples were characterized using X-ray diffraction (XRD, BRUKER, D8 ADVANCE A25 X) and scanning electron microscopy (SEM, Hitachi S4800) equipped with

EDS. XRD analysis was operated at 40 kV and 40 mA. Step scans were taken in the range of 2θ = 20–80 ° with a 0.02-step, 0.1 º s^{-1} scan speed and a 2 s exposure.

3. Results

Figure 1 shows the XRD patterns of the coated samples before and after the wet oxidation for 10 h. The results showed that the PIRAC prepared Cr_3Si-Cr_7C_3 outer layer was mainly composed of Cr_3Si, Cr_7C_3 along with a small amount of Cr_3C_2. It can be seen that after the wet oxidation at 700 ºC and 900 ºC, Cr_2O_3 was also detected in the Cr_3Si-Cr_7C_3/SiC/SiC coated samples. However, it should be noted that the ratio of the intensity of the Cr_2O_3 peak to that of the SiC peak was higher for sample oxidized at 900 °C compared to that oxidized at 700 °C. But no peaks due to oxides were detected for the SiC/SiC/SiC coated samples even after wet oxidation at 900 °C. After the wet oxidation at 1300 ºC, Cr_2O_3 and SiO_2 were detected in the Cr_3Si-Cr_7C_3/SiC/SiC coated samples. And the detected phases were mainly SiC and SiO_2 for the SiC/SiC/SiC coated samples.

Figure 2 shows the weight changes induced by wet oxidation for the coated samples. The SiC/SiC/SiC coated C/SiC composites exhibited continuous weight loss during the wet oxidation process and the weight loss decreased with increasing oxidation temperature. Moreover, during oxidation at 700 ºC and 900 ºC, the weight loss showed a linear relationship with respect to time for SiC/SiC/SiC coated C/SiC, whereas, for oxidation at 1300 °C, this variation followed a power law as shown in Fig. 2 (c) and can be described as follows:

$$\ln(\Delta w_{loss}) = 0.4782 \ln(t) - 2.9132 \quad (1a)$$

$$\text{i.e., } \Delta w_{loss} = 0.0543 \cdot t^{0.4782} \quad (1b)$$

where Δw_{loss} is the weight loss in mg cm^{-2}, and t is the time of oxidation in hours.

During the wet oxidation at 700 ºC and 900 ºC, the Cr_3Si-Cr_7C_3/SiC/SiC coated composite samples showed remarkably lower weight losses when compared to the SiC/SiC/SiC coated samples. During the wet oxidation at 700 ºC, the weight loss showed a linear relation with respect to time for the Cr_3Si-Cr_7C_3/SiC/SiC coated composite samples. During the wet oxidation at 900 ºC, the Cr_3Si-Cr_7C_3/SiC/SiC coated composite samples showed nonlinear weight loss, with a very rapid weight loss within the first 2 h followed by a gradual weight loss thereafter. During the wet oxidation at 1300 ºC, the Cr_3Si-Cr_7C_3/SiC/SiC coated composite samples showed non-linear weight gains, with a very rapid weight gain within the first 2 h followed by a gradual increase thereafter. Furthermore, during oxidation at 900 ºC and 1300 ºC, weight change vs time curves of the Cr_3Si-Cr_7C_3/SiC/SiC coated composite samples was well fitted by power function as shown in Fig. 2 (c) and Fig. 2 (d), respectively.

Figure 3 shows the surface morphology and area EDS results of the Cr_3Si-Cr_7C_3/SiC/SiC coated samples before and after the wet oxidation for 10 h. It can be seen that the surface morphology of the wet

oxidized samples was different to that of the as-received coating. The surface of the as-received Cr_3Si-Cr_7C_3 layer exhibited uniform folded ridge morphology as shown in Fig. 3 (a) and (b). After the wet oxidation at 700 ºC, the morphology changed significantly with the appearance of rough clusters as shown in Fig. 3 (c). A magnified view of the surface shown in Fig. 3 (d) indicated that the rough cluster was composed of fine lath-shaped particles. The EDS spectrum showed distinct oxygen and chromium peaks along with a weak carbon peak and the atomic percentages of C, O and Cr were 2.50, 52. 81 and 44.69, respectively. These results indicated the formation of a chromia film and there was chromium carbide remained. After the wet oxidation at 900 ºC, the surface showed a relatively flat morphology as shown in Fig. 3 (e). A magnified view shown in Fig. 3 (f) indicated that the surface was predominantly consisted of large platelets. The EDS spectrum showed only oxygen and chromium with atomic percentages of 57.05 and 42.95, respectively confirming that the surface was fully covered by chromia. After the wet oxidation at 1300 ºC, the surface showed an undulated loose morphology with a notable damage in the position of protrusion as shown in Fig. 3 (g). The magnified surface view showed however, that the sublayer was compact and composed of spherical particles. From the EDS spectrum, the surface composition was determined to be 1.51, 48.90, 5.19 and 44.40 at% of C, O, Si and Cr, respectively. These results revealed that the surface was covered mainly by chromia and silica films.

Figure 4 shows the surface morphology and area EDS results for the SiC/SiC/SiC coated samples before and after the wet oxidation for 10 h. When the oxidation temperature was 700 °C, the two samples showed similar surface morphologies and compositions as determined by area EDS. After the wet oxidation at 900 ºC, the surface morphology was similar to that of the as-received sample. The EDS results showed C, Si and O with an atomic percent of 48.51, 49.23 and 2.26, indicating the formation of a very thin silica layer on the surface. After the wet oxidation at 1300 ºC, the surface was covered by glassy material with a number of fine microcracks. The EDS results showed C, Si and O with an atomic percent of 3.51, 38.23 and 68.26, respectively, confirming that the surface was covered by silica.

Figure 5 shows the flexural strength of the coated samples before and after the wet oxidation for 10 h. After the wet oxidation, the SiC/SiC/SiC coated samples showed a lower residual flexural strength when compared to the Cr_3Si-Cr_7C_3/SiC/SiC coated samples. The values for average residual flexural strength of the SiC/SiC/SiC coated samples after 10 h oxidation at 700 ºC, 900 ºC and 1300 ºC were 275 MPa, 308 MPa, and 378 MPa, respectively, whereas, for Cr_3Si-Cr_7C_3/SiC/SiC coated samples, the corresponding values were 398, 400, and 409 MPa, respectively for the same temperatures. Taking into consideration the scatter in the values for strength, the residual flexural strength of the Cr_3Si-Cr_7C_3/SiC/SiC coated samples after the wet oxidation for 10 h was nearly the same as that of the as-received samples (411 MPa). This high value for residual flexural strength suggested that the Cr_3Si-Cr_7C_3/SiC/SiC coating had favorable oxidation resistance in the wet oxidation environments.

Figure 6 shows the typical stress-displacement curves during flexural tests of the coated 2D C/SiC before and after the wet oxidation for 10 h. The failure behavior of the as-received 2D C/SiC composite was rather brittle, and exhibited a steep stress drop after the maximum load point. The failure behavior of the

Cr_3Si-Cr_7C_3/SiC/SiC coated samples after the wet oxidation for 10 h was similar to that of the as-received samples. After the wet oxidation at 700 ºC and 900 ºC for 10 h, the failure behavior of the SiC/SiC/SiC coated samples showed a gradual drop in stress after the maximum load point. Moreover, it should be noted that, after the wet oxidation at 700 ºC and 900 ºC for 10 h, the slope of the initial linear part of the stress-displacement curve of the SiC/SiC/SiC coated 2D C/SiC showed a clear decrease. This indicated that the elastic modulus of the oxidized SiC/SiC/SiC coated 2D C/SiC was reduced.

4. Discussion

Under the present experimental conditions, the possible reactions for the coated samples are as follows [15–22]:

$2C_{(s)} + O_{2(g)} \rightarrow 2CO_{(g)}$ (1)

$C_{(s)} + H_2O_{(g)} \rightarrow CO_{(g)} + H_{2(g)}$ (2)

$4Cr_3Si + 13O_{2(g)} \rightarrow 6Cr_2O_3 + 4SiO_2$ (3)

$4Cr_7C_3 + 27O_{2(g)} \rightarrow 14Cr_2O_3 + 12CO_{(g)}$ (4)

$2SiC + 3O_{2(g)} \rightarrow 2SiO_2 + 2CO_{(g)}$ (5)

$SiC + 3H_2O_{(g)} \rightarrow SiO_2 + 3H_{2(g)} + CO_{(g)}$ (6)

$2Cr_2O_3 + 3O_{2(g)} + 4H_2O_{(g)} \rightarrow 4CrO_2(OH)_{2(g)}$ (7)

$SiO_2 + 2H_2O_{(g)} \rightarrow Si(OH)_{4(g)}$ (8)

Above 500 ºC, carbon oxidized according reactions (1) and (2) showing weight loss [15]. Cr_3Si and Cr_7C_3 begin to be oxidized above 660 ºC to form Cr_2O_3 and thus lead to weight gains [16–18], according reactions (3) and (4), respectively. While SiC will be oxidized above 800 ºC according to reaction (5), or above 1127 ºC according the reaction (6) that results in weight gain [7]. On the other hand, in water vapor containing oxidizing environments, above 1100 ºC, the formed Cr_2O_3 can volatilize by further reacting with water vapor to form gaseous $Cr(OH)_x$ [19–22] according to reaction (7).

For the wet oxidation at 1300 ºC of the SiC/SiC/SiC coated C/SiC, as shown in Eq. 2, the exponent was 0.4782, which was close to 0.5, typical of parabolic kinetics. Moreover, as shown in Fig. 4 (d), the silica surface was smooth without pores, humps or bubbles. Therefore, it can be ascertained that the weight loss of the SiC/SiC/SiC coated C/SiC during the wet oxidation at 1300 ºC follows parabolic kinetics. As a result, under the present experimental conditions, (i.e. gas velocity of 3.0 cm s^{-1}, 10 vol. % H_2O, and at 1 atm), the volatilization of SiO_2 according to the reaction (8) was negligible [14].

The weight change of the C/SiC composite during oxidation was governed by the overall outcome of the competing reactions, and the crystallography of the oxidized samples depended on the wet oxidation temperature.

As the temperature was increased from 700 ºC to 1000 ºC, the width of the microcracks in the coating decreased as temperature increased [23]. Consequently, the diffusion of the oxidizing gases into the PyC interlayer through microcracks in the coating decreased with increasing oxidation temperature. As a result, the weight loss due to oxidation of carbon phases decreased with increasing oxidation temperature for both the coated samples. For a specific oxidation condition (i.e. temperature, oxidizing atmosphere and reactant), the oxidation rate was constant. Since the width of the largest microcracks in the top layer of the Cr_3Si-Cr_7C_3/SiC/SiC coating was lower than that in the top layer of the SiC/SiC/SiC coating (as shown in Fig. 7), the inward diffusion of oxidizing gases through the former was much lower. Thus, the Cr_3Si-Cr_7C_3/SiC/SiC coated composite samples showed significantly lower weight loss when compared to the SiC/SiC/SiC coated samples.

At 700 ºC, since the oxidation of both Cr_3Si and Cr_7C_3 was very slow, only a small amount of Cr_2O_3 was produced, and no SiO_2 was detected. Hence, the XRD spectrum showed Cr_3Si, Cr_7C_3 and a small amount of Cr_2O_3 were detected and C, O, and Cr were detected by EDS. On the other hand, the oxidation of carbon phase was faster than the oxidation of Cr_3Si and Cr_7C_3. Therefore, the Cr_3Si-Cr_7C_3/SiC/SiC coated composite samples showed a nearly linear weight loss. At 900 ºC, the oxidation of Cr_3Si and Cr_7C_3 became faster, which led to the increased formation of Cr_2O_3 and the growth of Cr_2O_3 whiskers and platelets [24]. The oxide layer became thicker with increasing time of oxidation. Thus, the ratio of the intensity of the Cr_2O_3 peak to that of the SiC peak was higher for the sample oxidized at 900 ºC when compared to that oxidized at 700 ºC. Correspondingly, the elements detected by EDS were O and Cr. However, due to the thick oxide layer, the inward diffusion of oxidizing gases slowed down first and then leveled out. As a result, the Cr_3Si-Cr_7C_3/SiC/SiC coated composite samples showed a nonlinear weight loss behavior, with a very rapid weight loss within the first 2 h followed by an apparently gradual weight loss thereafter. The very low weight loss indicating the consumption of carbon was limited to the sub-surface region. At 1300 ºC, enhanced oxidation of the coating led to the rapid closure of the narrow microcracks in the outer layer of the Cr_3Si-Cr_7C_3/SiC/SiC coating due to thermal expansion of the formed SiO_2 and Cr_2O_3 [25, 26]. Moreover, presence of SiO_2 scale was favorable to inhibit the diffusion of both Cr and O, leading to oxidation process slowed and a relative compact oxide scale formed underneath the external oxide scale [27]. Additionally, water vapor decreased the viscosity of silica [28, 29] and thus, the carbon phases were protected from oxidation. On the other hand, the formed Cr_2O_3 volatilized by further reacting with water vapor to form gaseous $Cr(OH)_x$ [19–22]. Despite the fact that the rapid formation and escape of gases made the oxide films locally bulged and damaged, the sublayer was a compact oxide layer and retained the Cr_3Si-Cr_7C_3/SiC/SiC coating (shown in Fig. 8). Therefore, the Cr_3Si-Cr_7C_3/SiC/SiC coated samples showed non-linear weight gains, with a very rapid weight gains within the first 2 h folled by an apparently gradual weight gains thereafter. And detected phases were Cr_2O_3 and SiO_2. Thus, after

the wet oxidation for 10 h, the composite Cr_3Si-Cr_7C_3/SiC/SiC coated composite samples showed nearly the same failure behavior and flexural strength as the as-received samples.

For the SiC/SiC/SiC coated C/SiC, high temperature water vapor enhanced the non-uniform oxidation consumption of carbon phases, which led to the formation of pipeline-shaped channels between the carbon fiber and the SiC matrix [17]. As a result, the strength of the fibers and the bonding between the fiber/interphase/matrix would be weakened. Thus the stress-displacement curves showed a gradual stress drop after the maximum load point. Moreover, the non-uniform consumption of carbon phase increased the porosity of the composites increased. It is well acknowledged that the elastic moduli of porous materials decrease with increasing porosity [30, 31]. Therefore, the oxidized composite showed a reduced elastic modulus demonstrated by the decrease in the slope of the initial linear part of the stress-displacement curve. Above 900 ºC, the microcracks in the SiC coating are gradually sealed both by thermal expansion and by the formed SiO_2, due to surface oxidation. However, even though the oxidation of SiC resulted initially in the formation of a protective SiO_2 layer and a consequent weight gain, the rapid oxidation of carbon resulted in rapid weight loss. Therefore, the weight loss of the SiC/SiC coated composite samples decreased with increasing oxidation temperatures, showing the same trend as the flexural strength.

The above results suggest that the Cr_3Si-Cr_7C_3/SiC/SiC coating has enhanced protection against wet oxidation. And this improved oxidation resistance originates from the rapid formation of a protective layer of Cr_2O_3 by oxidation of Cr_3Si and Cr_7C_3 below 1000 ºC,while the formation of more protective layer of SiO_2 by oxidation of Cr_3Si and SiC at higher temperatures. The work provides support for the preparation of oxidation resistant coatings, which in return are essential to improve the service performance of carbon fiber reinforced composites in high temperature oxidizing environments.

4. Conclusions

In the present work, oxidation behavior of a Cr_3Si-Cr_7C_3/SiC/SiC coated C/SiC was investigated in 18 vol. % O_2 + 72 vol. % N_2 + 10 vol. % H_2O under 1 atm and a gas flow rate of 3.0 cm s^{-1} at 700 ºC, 900 ºC and 1300 ºC, and compared with that of a SiC/SiC/SiC coated C/SiC composites. Based on the results and discussion, the following conclusions can be drawn,

1. After the wet oxidation for 10 h, the phases formed on the Cr_3Si-Cr_7C_3/SiC/SiC coating were Cr_2O_3 at 700 ºC and 900 ºC, and Cr_2O_3 and SiO_2 at 1300 ºC.
2. The Cr_3Si-Cr_7C_3/SiC/SiC coating showed enhanced oxidation protection that is attributed to the rapid formation of a protective Cr_2O_3 layer by oxidation of Cr_3Si and Cr_7C_3 below 1000 ºC, while the formation of a more protective SiO_2 layer by oxidation of Cr_3Si and SiC at higher temperatures. The SiC/SiC/SiC coated C/SiC composites exhibit continuous weight loss during the wet oxidation. Compared to the SiC/SiC/SiC coated composite, the Cr_3Si-Cr_7C_3/SiC/SiC coated C/SiC showed remarkably reduced weight loss during the wet oxidation at 700 ºC and 900 ºC. At 1300 ºC, the Cr_3Si-

Cr_7C_3/SiC/SiC coated C/SiC samples showed a very rapid weight gain within the first 2 h due to rapid formation of SiO_2 and Cr_2O_3 initially, followed by an apparently gradual weight gain thereafter due to the volatilization of the formed Cr_2O_3.

3. After the wet oxidation for 10 h, the residual flexural strength of the Cr_3Si-Cr_7C_3/SiC/SiC coated composites had almost the same value as that of the as-received composite. And the failure behavior of the Cr_3Si-Cr_7C_3/SiC/SiC coated samples after the wet oxidation for 10 h was similar to that of the as-received samples.

Declarations

Declaration of Competing Interest

The authors declare that they have no known competing financial interests or personal relationships that could have appeared to influence the work reported in this paper.

Acknowledgments

The authors gratefully acknowledge the financial support from the fund of the Creative Research Foundation of Science and Technology on Thermostructural Composite Materials Laboratory (grant No. 6142911020105).

Data Availability

The raw data required to reproduce these findings are available to download from http://da.doi.org/10.17632/5g8fcvdhmz.3

References

1. Naslain R, Christin F. SiC-matrix composite materials for advanced jet engines. *MRS Bull* 2003, **28**: 654–658.
2. Wei K, Cheng XM, Mo FH, et al. Design and analysis of integrated thermal protection system based on lightweight C/SiC pyramidal lattice core sandwich panel. *Mater Des* 2016, **111**: 435–444.
3. Swain J, Gaurav K, Singh D, et al. A brief review on ceramic matrix composites, it's attributes and it's utility in future generation gas turbine. *Inter J Innov Res in Sci Technol* 2014, **1**: 290–292.
4. Sommers A, Wang Q, Han X, et al. Ceramics and ceramic matrix composites for heat exchangers in advanced thermal system-a review. *Appl Therm Eng* 2010, **30**: 1277–1291.
5. Krenkel W. Carbon fiber reinforced CMC for high-performance structures. *Inter J App Ceram Technol* 2004, **1**: 188–200.

6. Jacobson NS. Corrosion of silicon-based ceramics in combustion environments. *J Am Ceram Soc* 1993, **76**: 3–28.
7. Opila EJ. Variation of the oxidation rate of silicon carbide with water-vapor pressure. *J Am Ceram Soc* 1999, **82**: 625–636.
8. Wu SJ, Cheng LF, Zhang LT, et al. Wet oxidation behaviors of Hi-Nicalon fibers. *Appl Surf Sci* 2006, **253**: 1447–1450.
9. Qin F, Peng LN, He GQ, et al. Oxidation kinetics and mechanisms of carbon/carbon composites and their components in water vapour at high temperatures. *Corros Sci* 2015, **90**: 340–346.
10. Naslain R, Guette A, Rebillat F, et al. Oxidation mechanisms and kinetics of SiC-matrix composites and their constituents. *J Mater Sci* 2004, **39**: 7303–7316.
11. Park DJ, Jung YI, Kim HG, et al. Oxidation behavior of silicon carbide at 1200 °C in both air and water–vapor-rich environments. *Corros Sci* 2014, **88**: 416–422.
12. Jeguirim M, Tschamber V, Brilhac J F. Kinetics and mechanism of the oxidation of carbon by NO_2 in the presence of water vapor. *Inter J Chem Kinet* 2009, **41**: 236–244.
13. Goujard S, Vandenbulcke L. The oxidation behavior of two- and three-dimensional C/SiC thermostructural materials protected by chemical-vapor-deposition polylayers coatings, *J Mater Sci* 1994, **29**: 6212–6220.
14. Wu SJ, Wang YG, Guo Q, et al. Oxidation protective silicon carbide coating for C/SiC composite modified by a chromium silicide-chromium carbide outer layer. *Mater Sci Eng A* 2015, **644**: 268–274.
15. Opila EJ. Oxidation and volatilization of silica formers in water vapor. *J Am Ceram Soc* 2003, **86**: 1238–1248.
16. Ma JH, Gu YL, Shi L, et al. Synthesis and oxidation behavior of chromium silicide (Cr_3Si) nanorods. *J Alloy Compd* 2004, **375**: 249–252.
17. Raj SV. A preliminary assessment of the properties of a chromium silicide alloy for aerospace applications. *Mater Sci Eng A* 1995, **192-193**: 583–589.
18. Kok YN, Hovsepian PEh. Resistance of nanoscale multilayer C/Cr coatings against environmental attack. *Surf Coat Technol* 2006, **201**: 3596–3605.
19. Jacob YP, Haanappel VAC, Stroosnijder MF, et al. The effect of gas composition on the isothermal oxidation behaviour of PM chromium. *Corros Sci* 2002, **44**: 2027–
20. Yamauchi A, Kurokawa K, Takahashi H. Evaporation of Cr_2O_3 in atmospheres containing H_2 *Oxid Met* 2003, **59**: 517–527.
21. Othman NK, Othman N, Zhang J, et al. Effects of water vapour on isothermal oxidation of chromia-forming alloys in Ar/$O_2$and Ar/H_2 *Corros Sci* 2009, **51**: 3039–3049.
22. Ehlers J, Young DJ, Smaardijk EJ, et al. Enhanced oxidation of the 9%Cr steel P91 in water vapour containing environments. *Corros Sci* 2006, **48**: 3428–3454.
23. Hatta H, Aoki T, Kogo Y, et al. High-temperature oxidation behavior of SiC-coated carbon fiber-reinforced carbon matrix composites. *Compos Part A* 1999, **30**: 515–520.

24. Hänsel M, Quadakkers WJ, Young DJ. Role of water vapor in chromia-scale growth at low oxygen partial pressure. *Oxid Met* 2003, **59**: 285–301.
25. Soleimani-Dorcheh A, Donner W, Galetz MC. On ultra-high temperature oxidation of Cr-Cr_3Si alloys: Effect of germanium. *Mater Corros* 2014, **65**: 1143–1150.
26. Huang D, Zhang MY, Huang QZ, et al. Preparation of a double layer SiC coating and its oxidation resistance at 1773 K. *Corros Sci* 2014, **87**: 134–140.
27. Tunthawiroon P, Li YP, Tang N, et al. Effects of alloyed Si on the oxidation behaviour of Co–29Cr–6Mo alloy for solid-oxide fuel cell interconnects. *Corros Sci* 2015, **95**: 88–99.
28. Karki BB, Stixrude L. First-principles study of enhancement of transport properties of silica melt by water. *Phys Rev Lett* 2015, **104**: 215901.
29. Wu SJ, Cheng LF, Zhang J, et al. Tension-tension fatigue damage characteristics of a 3D SiC/SiC composite in H_2O-O_2-Ar environment at 1300ºC. *Mater Sci Eng A* 2006, 4**35–436**: 412–417.
30. Chen ZW, Wang X, Giuliani F, et al. Microstructural characteristics and elastic modulus of porous solids. *Acta Metall* 2015, **89**: 268–277.
31. Singh S, Srivastava VK. Effect of oxidation on elastic modulus of C/C-SiC composites. *Mater Sci Eng A* 2008, **486**: 534–539.

Figures

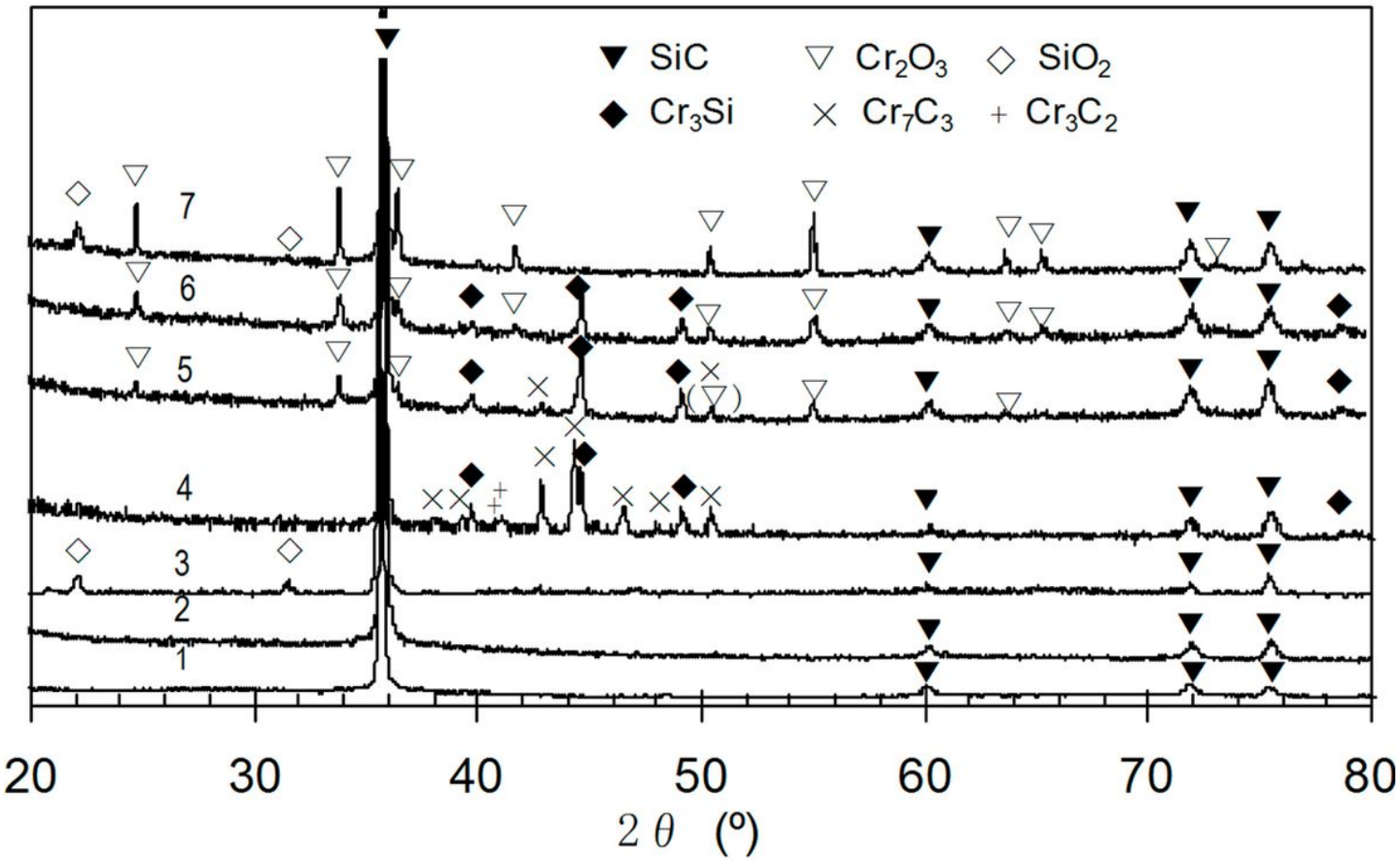

Figure 1

XRD patterns of the coated samples before and after the wet oxidation for 10h 1. as received SiC/SiC/SiC; 2. SiC/SiC/SiC 900 ºC; 3. SiC/SiC/SiC 1300 ºC; 4. As-received Cr3Si-Cr7C3/SiC/SiC; 5.Cr3Si-Cr7C3/SiC/SiC 700 ºC; 6. Cr3Si-Cr7C3/SiC/SiC 900 ºC; 7. Cr3Si-Cr7C3/SiC/SiC 1300 ºC

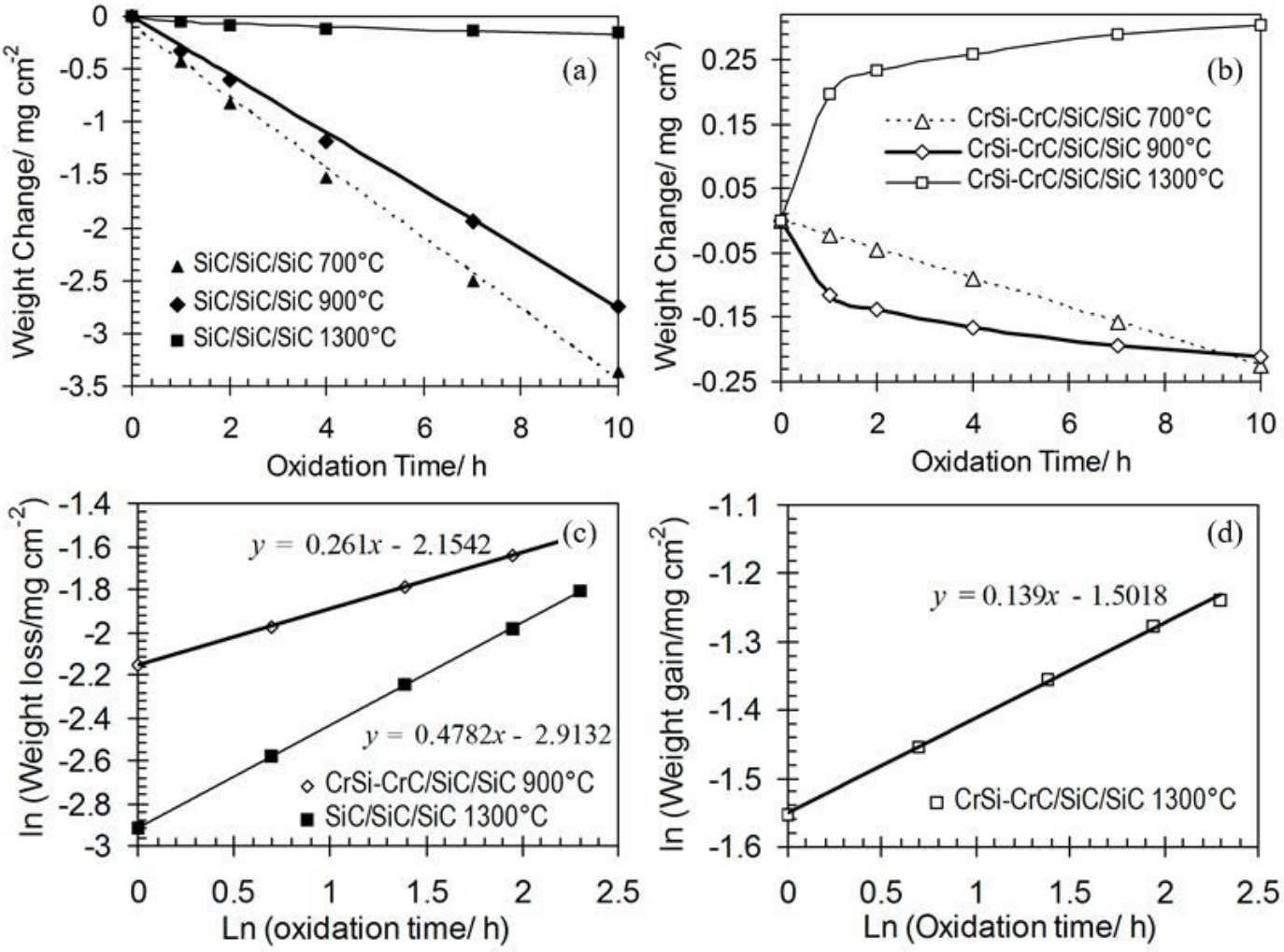

Figure 2

Weight change of the coated 2D C/SiC composite during the wet oxidation

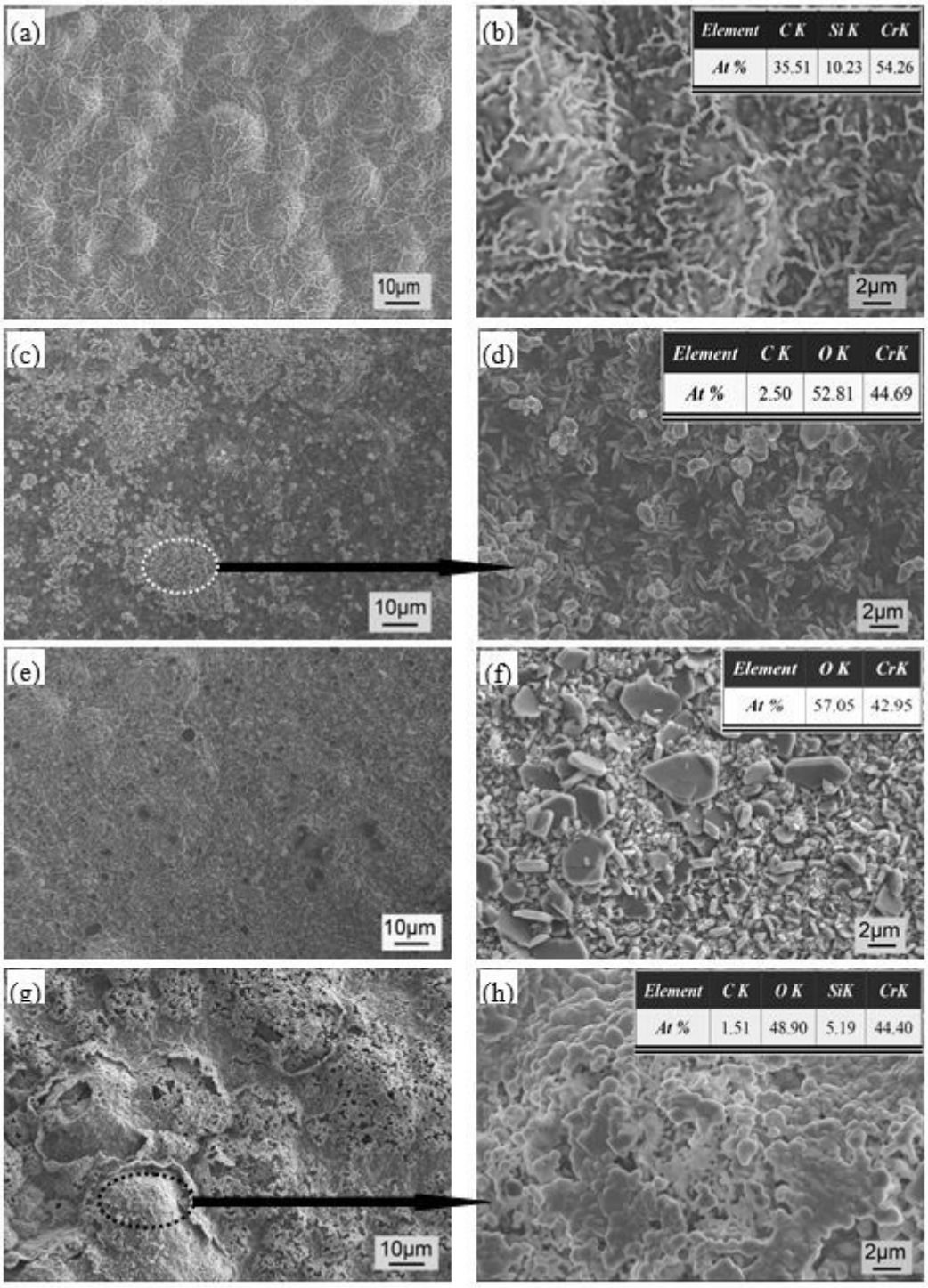

Figure 3

Surface morphology and EDS results of the Cr3Si-Cr7C3/SiC/SiC coated samples before and after the wet oxidation for 10h (a) as-received coating; (b) magnified view of (a); (c) after the wet oxidation at 700 ºC; (d) magnified view of (c); (e) after the wet oxidation at 900 ºC; (f) magnified view of (e); (g) after the wet oxidation at 1300 ºC; (h) magnified view of (g)

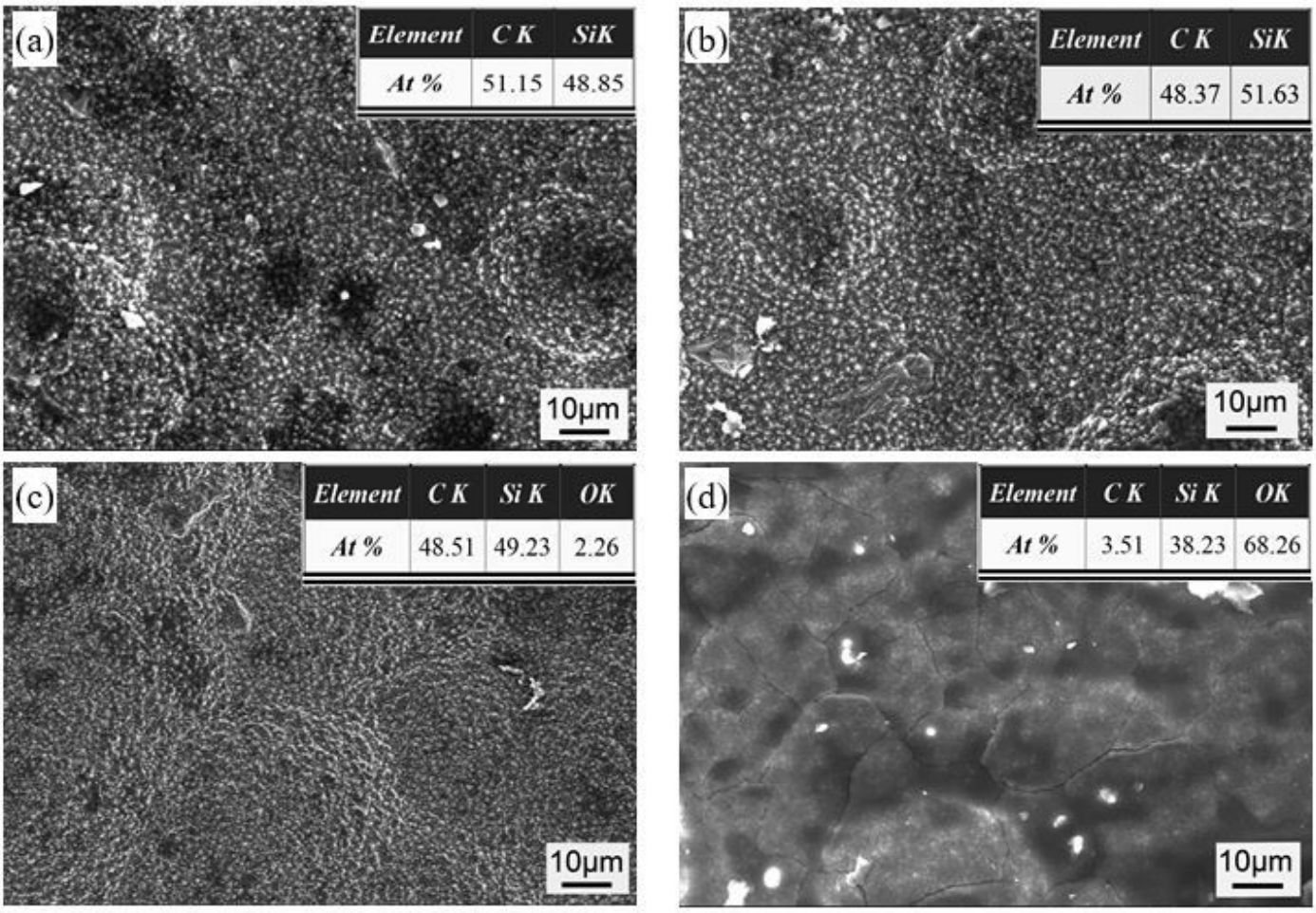

Figure 4

Surface morphology and EDS results of the SiC/SiC/SiC coated samples before and after the wet oxidation for 10h (a) as-received coating; (b) after the wet oxidation at 700 ºC; (c) after the wet oxidation at 900 ºC; (d) after the wet oxidation at 1300 ºC

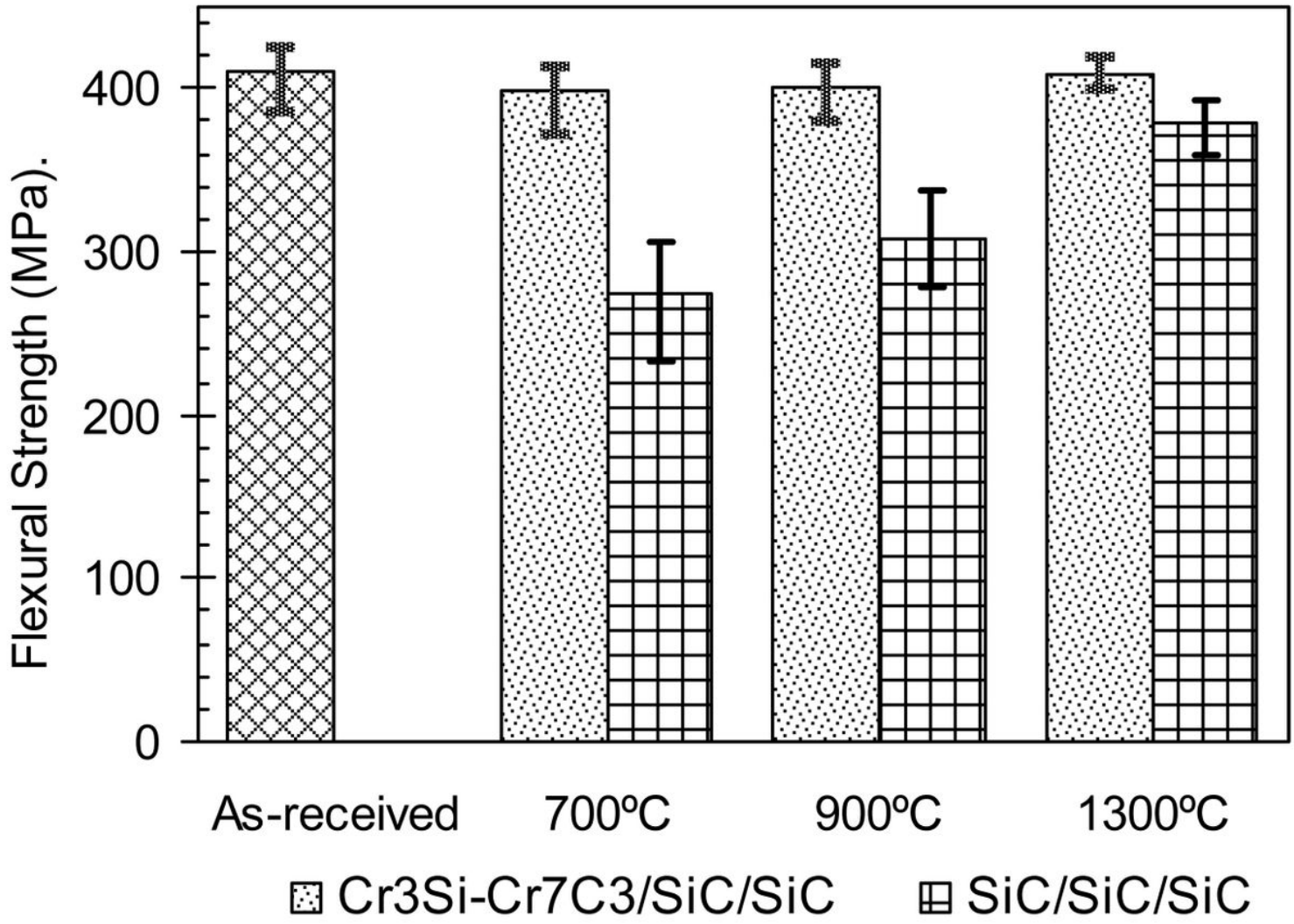

Figure 5

Flexural strength of the coated 2D C/SiC before and after the wet oxidation for 10h

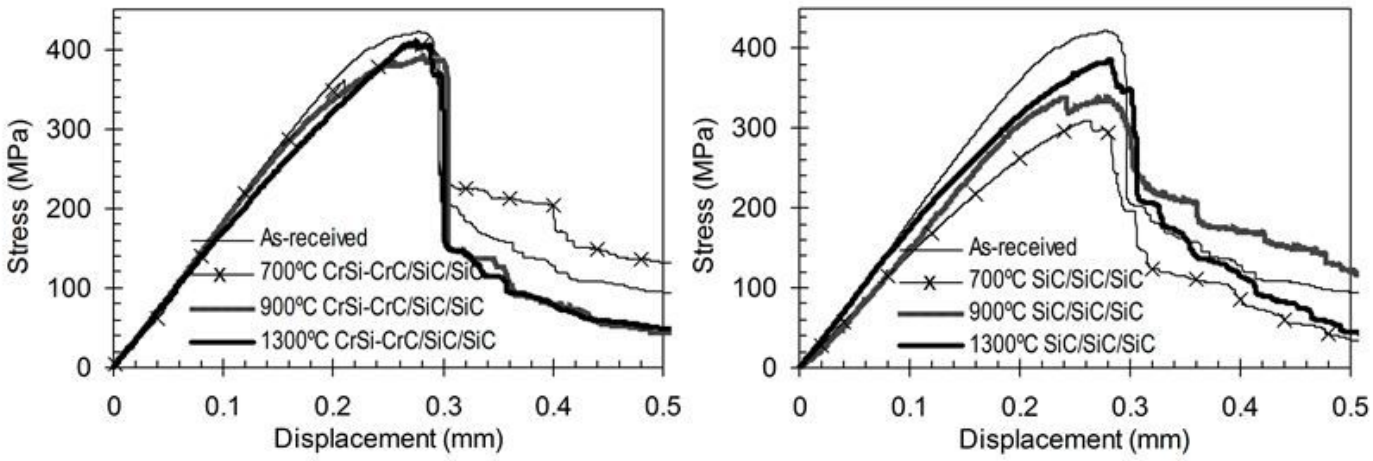

Figure 6

Typical flexural stress-displacement curves of the coated 2D C/SiC before and after the wet oxidation for 10h

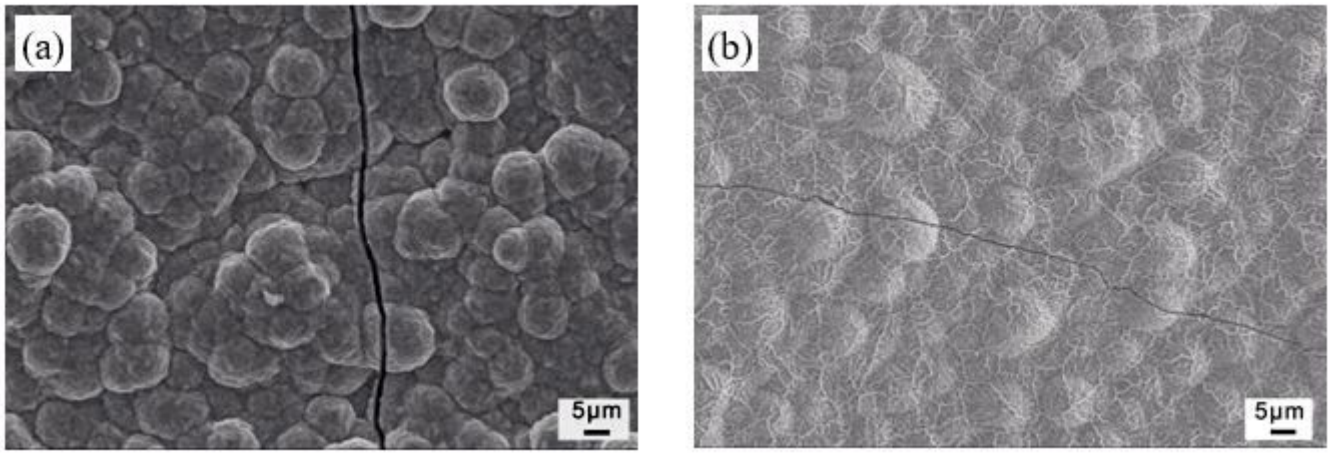

Figure 7

The largest microcracks in the top layer of the coating of (a) SiC/SiC/SiC; (b) Cr3Si-Cr7C3/SiC/SiC

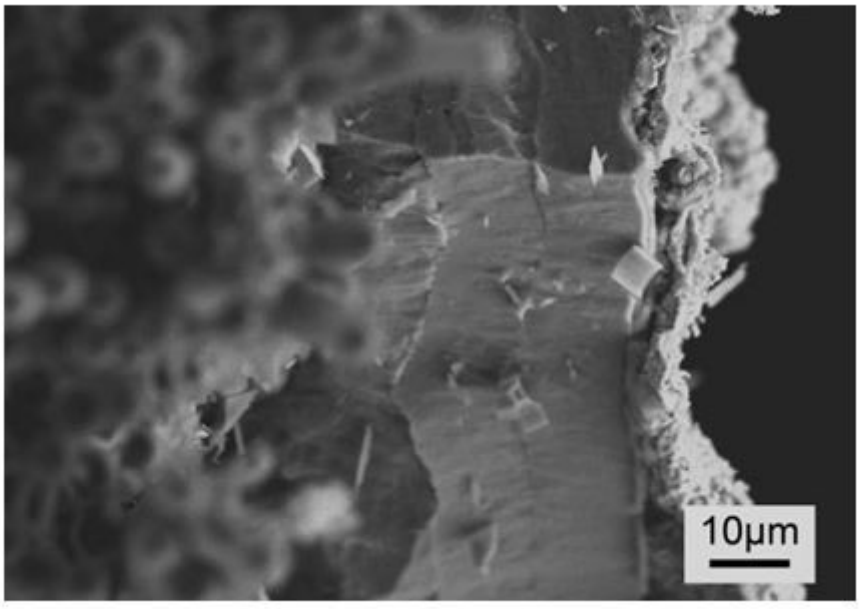

Figure 8

Cross-section morphologies of the Cr3Si-Cr7C3/SiC/SiC coating after the wet oxidation at 1300 ºC for 10h.